



Cite this: *J. Mater. Chem. C*, 2016, 4, 1194

The effect of tuning the microstructure of TIPS-tetraazapentacene on the performance of solution processed thin film transistors†

Fabian Paulus,^a Jens U. Engelhart,^a Paul E. Hopkinson,^{bc} Christian Schimpf,^d Andreas Leineweber,^d Henning Sirringhaus,^e Yana Vaynzof^{bc} and Uwe H. F. Bunz^{*ae}

We report a comprehensive study of the symmetrical 6,13-bis((triisopropylsilyl)ethynyl)tetraazapentacene (**TIPS-TAP**) used as an electron transporting material in organic field-effect transistors. We study the optical, electronic, structural and morphological properties of thin films of **TIPS-TAP** as deposited by spin-coating and zone-casting techniques. Depending on the solution processing conditions and procedures we find a variety of microstructures for **TIPS-TAP** ranging from highly polycrystalline to well-aligned crystalline films. Field-effect transistors are fabricated in two different architectures to evaluate the charge transport properties of **TIPS-TAP** in such films, and bias-stress experiments reveal a good electric stability of **TIPS-TAP**. The extracted electron mobilities vary over several orders of magnitude depending on the resulting morphology of the active layer reaching a maximum of $0.42 \text{ cm}^2 \text{ V}^{-1} \text{ s}^{-1}$ for uniaxial aligned crystallites in zone-cast transistors.

Received 14th October 2015,
Accepted 3rd January 2016

DOI: 10.1039/c5tc03326h

www.rsc.org/MaterialsC

Introduction

Small molecules as organic semiconductors in organic field-effect transistors (OFETs) were extensively studied in the past decades.^{1,2} The high solubility of these materials in organic solvents offers the possibility of low temperature solution processing and large-area fabrication on a huge variety of different substrates potentially leading to low-cost electronics.^{3,4} Pentacene is an extensively studied small molecule and shows high hole mobilities in thin film transistors. Its chemical stability was significantly increased by the introduction of triisopropylsilyl ethynyl (TIPS) side groups by Anthony *et al.* (Fig. 1).⁵ These groups not only prevent the oxidation of the pentacene core, they also increase the solubility of the aromatic molecule and change its molecular packing in the solid state.

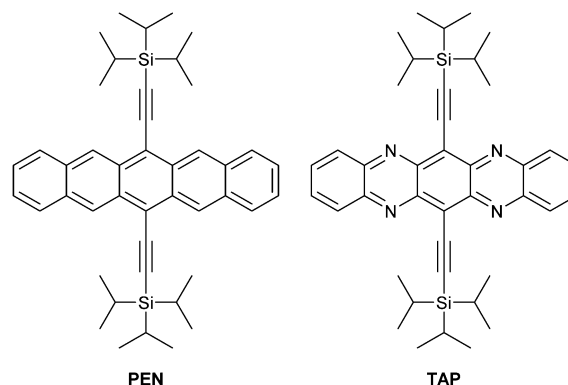


Fig. 1 Molecular structure of 6,13-bis((triisopropylsilyl)ethynyl)pentacene (**TIPS-PEN**) and 6,13-bis((triisopropylsilyl)ethynyl)-5,7,12,14-tetraazapentacene (**TIPS-TAP**). The side chains make the molecules soluble and increase their stability towards oxidation in air.

^a Universität Heidelberg, Organisch-Chemisches Institut, Im Neuenheimer Feld 270, 69120 Heidelberg, Germany. E-mail: uwe.bunz@oci.uni-heidelberg.de

^b Universität Heidelberg, Kirchhoff-Institut für Physik, Im Neuenheimer Feld 227, 69120 Heidelberg, Germany

^c Universität Heidelberg, Centre for Advanced Materials, Im Neuenheimer Feld 225, 69120 Heidelberg, Germany

^d TU Bergakademie Freiberg, Institut für Werkstoffwissenschaft, Gustav-Zeuner-Str. 5, 09599 Freiberg, Germany

^e University of Cambridge, Cavendish Laboratory, J J Thomson Avenue, Cambridge CB3 0HE, UK

† Electronic supplementary information (ESI) available: Synthesis and purification of **TIPS-TAP**, thin films and device preparation, optical micrographs for zone-cast and polycrystalline films on glass and BCB, detailed XRD data and additional FET characteristics. See DOI: 10.1039/c5tc03326h

Solution processed OFETs of **TIPS-PEN** with various morphologies and electronic performances have been reported in the recent years and hole mobilities from 0.1 up to $1.5 \text{ cm}^2 \text{ V}^{-1} \text{ s}^{-1}$ were reported for polycrystalline films of **TIPS-PEN** from solution processing.^{2,6–8} Slow deposition techniques like zone-casting or shear coating allow fine control of the crystallisation process and the resulting uniaxial aligned crystalline films. Some authors report hole mobilities of $>10 \text{ cm}^2 \text{ V}^{-1} \text{ s}^{-1}$.^{9–12} In addition, electron transport in pentacene can be observed if low work-function electrodes such as calcium are chosen as the contact material.^{13,14} Another possibility, to achieve n-type transport is the energetic stabilisation of the

frontier molecular orbitals (FMO) *via* chemical modification. The introduction of nitrogen in the aromatic backbone of pentacene derivatives lowers the energy of their highest occupied and lowest unoccupied molecular orbitals (HOMO and LUMO), resulting in excellent electron injection even from gold electrodes.^{15–18} These azaacenes are a class of small molecules that show excellent stability and solubility and can exhibit high charge carrier mobilities, necessary for high performance OFETs.^{15,16} Several nitrogen containing acenes were reported as active layer in field-effect transistors demonstrating that azaacenes are valuable electron transporting materials with good performance and stability. Electron mobility values typically range from 0.1–0.4 cm² V^{−1} s^{−1} for different derivatives and processing methods.^{18–22} The highest electron mobility values for the azaacenes have been reported for the soluble tetraazapentacene (**TIPS-TAP**), first synthesised in 2009 by Bunz and coworkers (Fig. 1).²³ **TIPS-TAP** shows a very similar packing motif (brickwork pattern) as **TIPS-Pentacene** (**TIPS-PEN**) and is also highly soluble and crystallises well from a variety of organic solvents.^{5,23}

TIPS-TAP was first investigated in thin film transistors by Miao and co-workers. For vacuum deposited **TIPS-TAP** on silicon dioxide surfaces modified with trichloro(octadecyl)silane (OTS), the authors reported mobilities up to 3.3 cm² V^{−1} s^{−1}.²² Alternatively, drop-casting on tailored self-assembled monolayers of phosphonic acids deposited on thin aluminium titanium oxides enhanced the mobility up to 5.0 cm² V^{−1} s^{−1}.^{24,25} Despite these promising values, the authors did not discuss the electric stability and hysteresis of their transistors. Additionally, the above mentioned deposition methods are rather slow and are unsuitable for high-throughput fabrication processes.

Here we report the fabrication of thin film transistors of **TIPS-TAP** based on spin-coating and zone-casting techniques. While spin-coating results mostly in polycrystalline films, zone-casting can be used to finely control the crystallisation process of **TIPS-TAP** and produces well-oriented large crystallites on the substrates. In each case, the resulting microstructure is correlated to the performance in OFETs. We investigate the energetics in thin film, as well as the morphology and electron transport properties of **TIPS-TAP** under a variety of solution processing conditions. Finally, the current–voltage characteristics of the fabricated transistors are discussed in context of their hysteresis and electric stability.

Results and discussion

TIPS-TAP was synthesised following the reported procedure from Liu *et al.* using Grignard precursors for the introduction of the side chains (see ESI†).²⁴ This synthetic route results in slightly higher yields than the originally employed route *via* the organo lithium precursors and the reduction with sodium hypophosphite.²³ The fully oxidised **TIPS-TAP** was carefully purified following several steps of recrystallization from hexane and ethanol. Further purification through sublimation fails as the sublimated material contains impurities afterwards. Attempts of a thin film deposition *via* thermal evaporation at low pressure

($\sim 10^{-5}$ mbar) also resulted a film of **TIPS-TAP** that contained impurities. The residual as well as the sublimed material show traces of impurities (see ESI†) and cannot be used for device fabrication. The nature of the impurities remains unclear. Our inability to produce pure **TIPS-TAP** films by thermal evaporation stresses the importance of investigating this material in solution processed OFETs.

Although efficient electron injection into **TIPS-TAP** has been demonstrated previously from both gold and silver, conflicting values of the energy levels of **TIPS-TAP** were reported. DFT calculations (B3LYP 6-31G**//B3LYP 6-31G**) in the gas phase predicted the HOMO and LUMO energies to be −5.29 eV and −3.43 eV, respectively.²³ Cyclic voltammetry in solution determined the LUMO level to be −4.01 eV.^{22,23} In combination with the experimentally determined optical gap the HOMO level was found to be −5.75 eV. These measurements do not represent the energy levels of **TIPS-TAP** in the solid state and also do not allow accurate analysis of the electron injection barrier. Therefore we performed ultraviolet photoemission spectroscopy (UPS) measurements on **TIPS-TAP** films spin-coated on gold (Fig. 2b). We interpret the onset of the low binding energy edge of the valence band as the position of the HOMO, measured to be 6.05 eV below the vacuum level. As expected, the nitrogen substitution in the aromatic backbone leads to a stabilisation of the HOMO as compared to that of spin-coated **TIPS-PEN** (5.04 eV).²⁶ Additionally, compared to the values obtained from cyclic voltammetry measurements the energy levels of **TIPS-TAP** in the solid state are considerably stabilised in agreement with previous studies on **TIPS-PEN**,²⁷ demonstrating the importance of electronic energy level characterisation in the solid state for FET applications.

The absorption of **TIPS-TAP** in thin film is broadened and red-shifted compared to the absorption in solution (Fig. 2a). The determination of the optical gap is complicated by the broad absorption into the near IR, introducing a larger error in

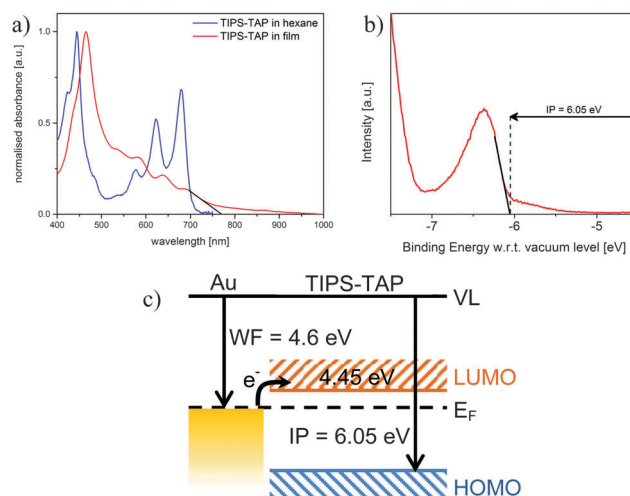


Fig. 2 (a) UV-vis absorption of **TIPS-TAP** in solution and thin film, (b) UPS low binding energy edge of a thin film of **TIPS-TAP** on a gold substrate, (c) schematic energy level diagram for **TIPS-TAP**/Au.

our measurements. Due to the absorption onset in thin films of **TIPS-TAP** ($\lambda_{\text{onset}} = 770$ nm) the optical gap is determined to be (1.6 ± 0.1) eV. Assuming that the transport gap is similar to the optical gap, the resulting LUMO position is found to be (-4.45 ± 0.1) eV. Electron injection should be easily achieved from gold electrodes.

The choice of both substrate and solvent affect the morphology of the spin-coated films of **TIPS-TAP**. Spin-coating solutions of **TIPS-TAP** on glass results in rough and discontinuous polycrystalline films (see ESI†). The addition of a polyimide interlayer improves the wettability of the organic solution and a spherulitic growth of **TIPS-TAP** is observed for all solvents used in this study, similarly to films of **TIPS-PEN** in high-performance solution processed OFETs.⁸ The domain size of these **TIPS-TAP** spherulites can be tuned by the choice of solvent. While films deposited from toluene exhibit small domain sizes of 30–50 μm , tetralin results in spherulitic structures with diameters up to millimetre size (Fig. 3). The rms-roughness of these spin-coated films is below 10 nm, suitable for top-gate transistors. The large domains for tetralin are smooth with an rms below 3 nm (Fig. 4). Alternatively, spin-coated films prepared on a cross-linked benzocyclobutene (BCB) interlayer exhibit a very similar morphology, although the domain size is slightly smaller (see ESI†).

Prior to application of **TIPS-TAP** in field-effect transistors we confirmed that the polycrystalline films deposited by spin-coating exhibit the same solid state packing as found for single crystals grown from hexane solution. The X-ray diffraction (XRD) patterns are in good agreement with those previously reported on drop-cast and vacuum deposited films.^{22,24,25} The observed diffraction patterns always show a similar background intensity, which can be ascribed to the glass/polyimide substrate but also Laue fringes from the small angle scattering regions and the Bragg reflections. The relative intensities and position of the four visible Bragg reflections are in good agreement with the $(00l)$ reflections, with $l = 1, 2, 3$ and 5 of the reported single-crystal structure of **TIPS-TAP** (Fig. 5).²³ Occurrence of only these reflections implies a strong preferred orientation of the

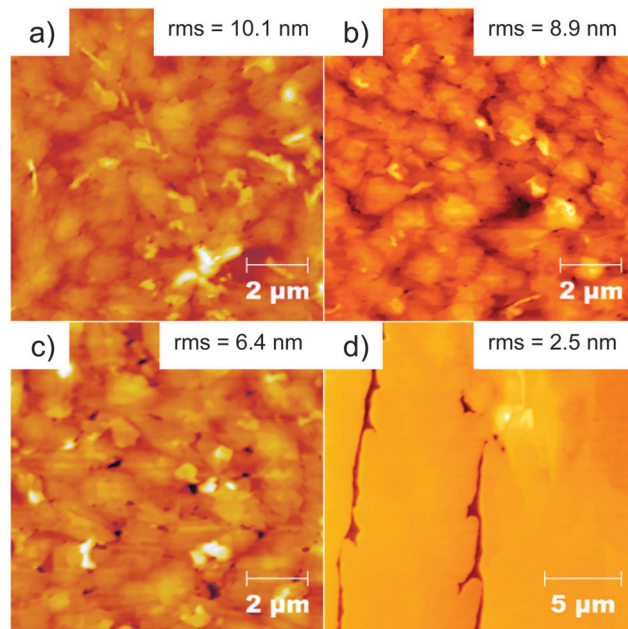


Fig. 4 AFM height micrographs of polycrystalline films of **TIPS-TAP** cast from different solvents on polyimide: (a) toluene, size $10 \times 10 \mu\text{m}^2$; (b) chlorobenzene, $10 \times 10 \mu\text{m}^2$; (c) *m*-xylene, $10 \times 10 \mu\text{m}^2$; (d) tetralin, $20 \times 20 \mu\text{m}^2$.

crystallites with the $(001)/(00l)$ planes parallel to the substrate. The d-spacing of all four reflections consistently agrees with the single-crystal based structural data ($d_{(001)}$ calculated as 16.50 Å). Films deposited from tetralin exhibit the strongest Bragg reflections likely due to a more pronounced preferred orientation of the crystallites in the polycrystalline film which is in good agreement with the morphological studies above. As expected, spin-coated films of **TIPS-TAP** exhibit the same $(00l)$ -orientation as **TIPS-PEN** in high performing OFET.⁶ In addition, deposition by spin-coating does neither change the type of polymorph nor the preferred orientation and thus not the molecular orientation of **TIPS-TAP** compared to that previously reported for vacuum deposited and drop-cast films. The $d_{(00l)}$ -spacing values of 16.53 Å and 16.56 Å reported for vacuum deposited and drop-cast films are marginally larger than encountered here.^{22,24,25}

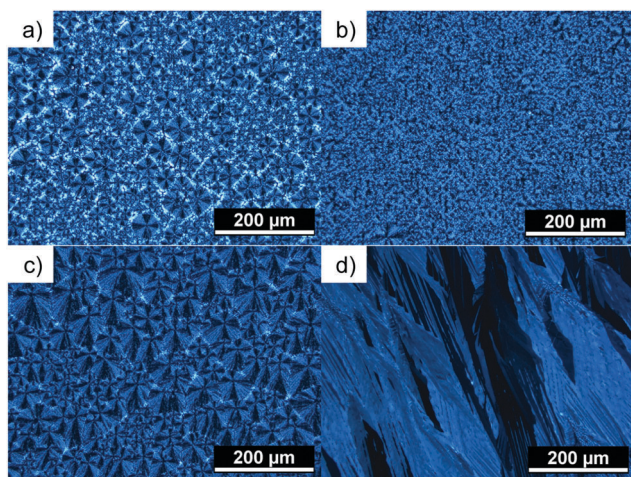


Fig. 3 Images of thin films of **TIPS-TAP** under crossed polarisers spin-coated from different solvents: (a) toluene; (b) chlorobenzene; (c) *m*-xylene; (d) tetralin.

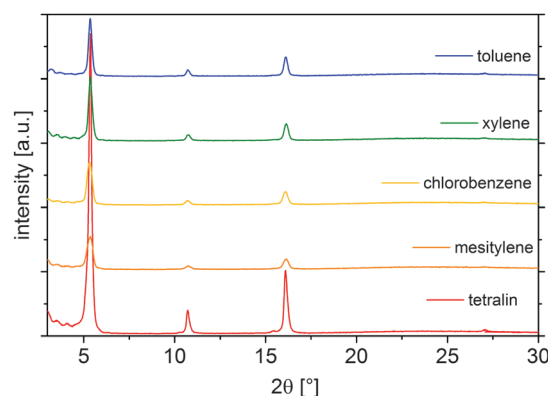


Fig. 5 XRD-pattern of a polycrystalline film of **TIPS-TAP** spin-coated from various solvent on polyimide.

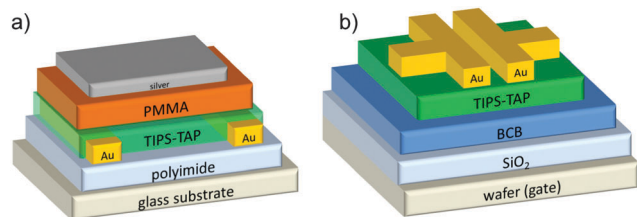


Fig. 6 Schematic architectures for field-effect transistors fabricated with **TIPS-TAP** as semiconductor (a) bottom-contact/top-gate (BC/TG) and (b) bottom-gate/top-contact transistor (BG/TC).

Field-effect transistors of **TIPS-TAP** were fabricated in two architectures. For bottom-contact top-gate (BC/TG) transistors gold electrodes with different W/L ratios were patterned on polyimide coated glass slides using a double resist photolithography process. **TIPS-TAP** was spin-coated from different organic solvents and topped with a layer of PMMA, followed by a thermal evaporation of the silver gate electrode (Fig. 6a). Bottom-gate top-contact (BG/TC) FETs were prepared by spin-coating of **TIPS-TAP** on a cross-linked BCB layer on doped silicon/silicon dioxide wafers.²⁸ The top contacts (gold) were evaporated through a shadow mask (Fig. 6b).

In contrast to the work of Miao and coworkers the transistors were characterised in a nitrogen filled glovebox with low humidity and low oxygen concentrations rather than in vacuum. Our test conditions better represent the environment for a possible application of this material. Sweep rate and measurement

conditions were adjusted to avoid an overestimation of the electron mobility due to charging or internal dynamic processes within the devices. The bottom-contact top-gate architecture was utilized to investigate the influence of the choice of solvent on the electrical properties of the polycrystalline films of **TIPS-TAP**. Based on the low injection barrier for electrons from gold the fabricated devices show, as expected, a clear transport of electrons as majority charge carrier. Even though the devices are not measured in vacuum, the hysteresis of our devices is low (Fig. 7). Both the extracted average and best electron mobilities increase with the higher boiling point of the organic solvent used for deposition, reaching a maximum value of $0.31 \text{ cm}^2 \text{ V}^{-1} \text{ s}^{-1}$ for tetralin. This is in excellent agreement with the increase of the domain sizes of the spherulites discussed above. The electrical parameters and averaged mobilities of the devices fabricated in the bottom-contact top-gate architecture are summarised in Table 1.

We note that in the bottom-contact architecture some non-linear contact limitations were observed (see Fig. 7a). We propose that the observed limitations in charge injection for such **TIPS-TAP** devices are based on the (001)-orientation of the films that hinder good injection of electrons into the aromatic π -system. This suggests that the mobility values extracted from a linear fit of the square root plot of the channel current in the saturation regime might overestimate the electron mobility of these devices. To resolve this issue we have fabricated devices in a bottom-gate top-contact architecture using a high-boiling point solvent. In this BG/TC architecture the non-linear contact

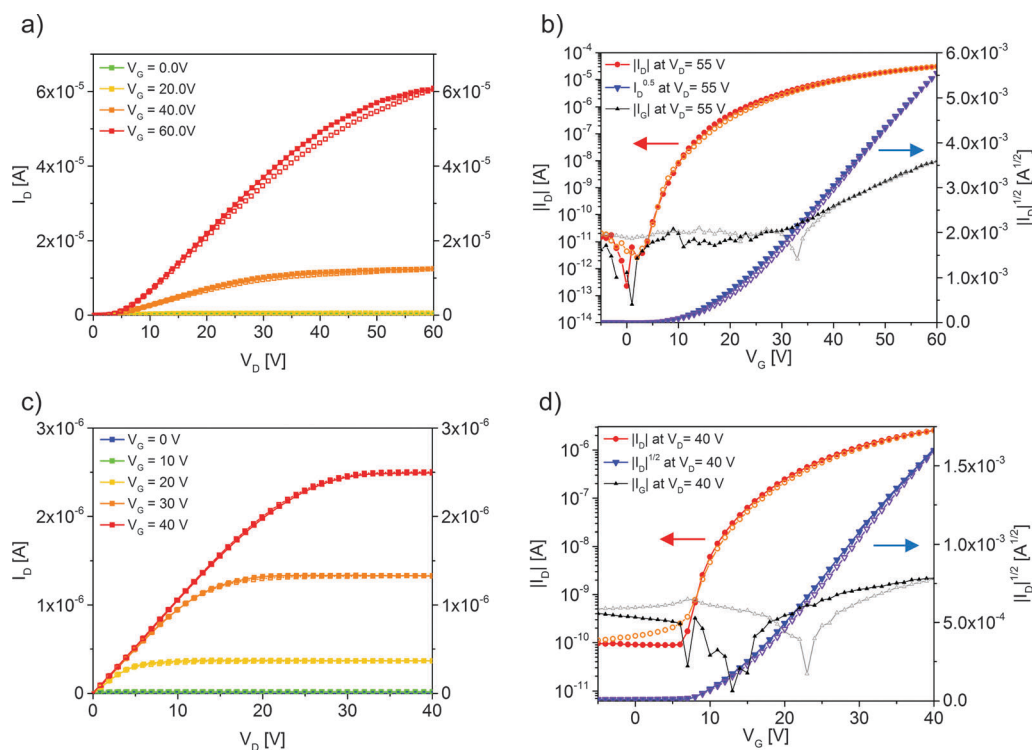


Fig. 7 I - V -characteristics (forward sweep – filled/backward sweep – open symbols) of representative transistors of **TIPS-TAP**; (a) output and (b) transfer characteristic of a bottom-contact top-gate FET with **TIPS-TAP** spin-coated from tetralin on polyimide with $W = 1000 \text{ }\mu\text{m}$ and $L = 10 \text{ }\mu\text{m}$. (c) Output and (d) transfer characteristic of a bottom-gate top-contact FET with **TIPS-TAP** spin-coated from mesitylene on BCB with $W = 1500 \text{ }\mu\text{m}$ and $L = 130 \text{ }\mu\text{m}$ (gate leakages in the background).

Table 1 Summarized electric parameters for field-effect transistors fabricated from spin-coated **TIPS-TAP**. Averaged values and standard errors were obtained from a representative set of identically prepared transistors. On/off-ratios ($I_{\text{on}}/I_{\text{off}}$) were calculated for $I_{\text{on}}(V_G = 0 \text{ V})/I_{\text{off}}(V_G = 40 \text{ V})$

| Solvent | Boiling point [°C] | Best μ_e [$\text{cm}^2 \text{V}^{-1} \text{s}^{-1}$] | Average μ_e [$\text{cm}^2 \text{V}^{-1} \text{s}^{-1}$] | Average threshold voltage [V] | On/off ratio |
|---------------|--------------------|---|--|----------------------------------|-----------------|
| Toluene | 111 | 0.005 | $(2.7 \pm 0.5) \times 10^{-3}$ | 5 ± 3 | 10^3 – 10^4 |
| Chlorobenzene | 131 | 0.07 | $(3.3 \pm 1.2) \times 10^{-2}$ | 10 ± 3 | 10^4 |
| Xylene | 139 | 0.09 | $(4.0 \pm 0.7) \times 10^{-2}$ | 10 ± 1 | 10^3 |
| Tetralin | 208 | 0.31 | $(1.0 \pm 0.3) \times 10^{-1}$ | 25 ± 2 | 10^5 – 10^6 |

behaviour is not observed (see Fig. 7c), probably due to the more intimate nature of the contact between Au and **TIPS-TAP**. In this architecture, an average electron mobility is found to be $(5.8 \pm 0.3) \times 10^{-2} \text{ cm}^2 \text{V}^{-1} \text{s}^{-1}$, which is in agreement with average values calculated previously for the BC/TG architecture. These results demonstrate that the non-linear contact effects do not result in a gross overestimation of the electron mobilities (see ESI†) and that the obtained values are representative of spin-coated OFETs of **TIPS-TAP**.

Independent of device architecture, none of our OFETs exhibit significant hysteresis, indicating a well-designed interface between **TIPS-TAP** and the dielectric. In particular, the reverse-sweep of the transfer curves demonstrates that no dynamic trapping of charges affects the device performance. However, we note that the charge carrier mobilities for all our devices are significantly lower than those previously reported in literature for **TIPS-TAP** by Miao and co-workers, and suggest three factors that may account for this disparity. Firstly, due to the combination of thicker dielectric layers and the applied gate voltages, the fabricated devices were run at lower charge carrier densities compared to literature. This lower carrier density may result in the charge transport occurring in the low energy tail of the transport states. Secondly, the microstructure of spin-cast films exhibits more grain boundaries than that of drop-cast layers, which in turn may limit the device performance. Finally, the environment and other measurement parameters may play a role in the observed performance. Measurements under vacuum conditions might be superior to those in nitrogen. On the other hand, the transfer characteristics of the drop-cast/evaporated OFETs of Miao *et al.* often show bending which could indicate possible contact issues, charge trapping or a high gate leakage.^{3,22,24,25} Gate leakage is also observed in output characteristics where a negative source drain current is observed at $V_{\text{DS}} = 0 \text{ V}$. Without further information on the gate leakage and reverse sweeps of these previously reported devices, one cannot determine the cause of the disparity.

To investigate whether morphology plays a significant role in determining the performance of the **TIPS-TAP** OFETs, we employed the zone-casting technique to grow crystalline uniaxially oriented highly crystalline films.^{9,29,30} Mesitylene was used for this study, as it provides both good wettability and solubility. Films for transistors were prepared on the same substrates used for spin-coating under nitrogen atmosphere. The resulting films show well-oriented crystalline ribbons of various widths and length of over a centimetre.

The obtained crystalline ribbon films look similar to the drop-cast structures from Miao *et al.* but cover the full substrate.²⁴ The thickness of the ribbons is adjusted based on the concentration, temperature and casting speed used for deposition and was

chosen to be between 50–75 nm. The pre-structured or evaporated gold electrodes were oriented perpendicular to the zone-casting direction (Fig. 8). Despite the significant decrease in the number of grain boundaries, the zone-cast transistors exhibit only slightly higher electron mobilities than the spin-coated ones (see Table 2). The highest electron mobility achieved with zone-casting is $0.42 \text{ cm}^2 \text{V}^{-1} \text{s}^{-1}$ and is in the same order of magnitude as the electron mobilities obtained from spin-coated tetralin films. This similarity implies that the morphology resulting from spin-coating using a high boiling point solvent is close to the optimised morphology that can be obtained by controlled crystallization in the case of zone-casting. The observation that the zone-casting technique does not result in a significant enhancement of the electron mobility values is unexpected and is subject to further investigations.

Finally, we investigated the stability of **TIPS-TAP** BG/TC-transistors to electrical stress under nitrogen atmosphere. The transistors were biased at $V_G = V_D = 40 \text{ V}$ (saturation) for 20 minutes, and immediately afterwards a transfer characteristic in the saturation regime ($V_D = 50 \text{ V}$) was recorded. After a recovery time (*ca.* 40 min), the device was re-stressed beginning the next cycle of measurement. After every fifth cycle of stressing and transfer characterisation, an output characteristic was recorded to monitor variations in injection. The FETs remained operational for over 25 of these cycles (>900 minutes), with only a slight decrease in channel current due to an increase in threshold voltage (Fig. 9). No variation in the injection behaviour was observed in the

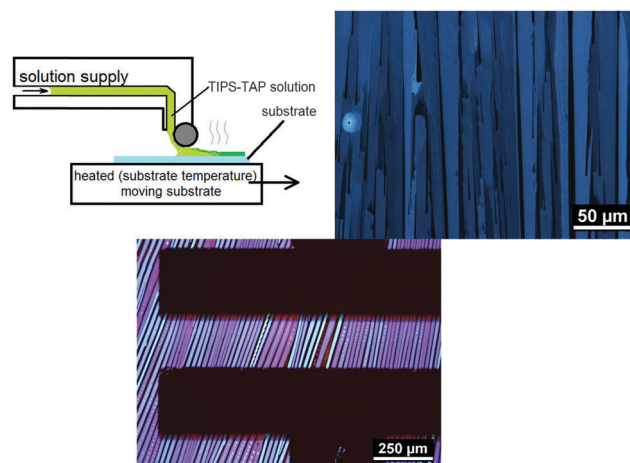


Fig. 8 Schematic principle of the zone-casting deposition (top left). Uniaxially orientated crystallites of **TIPS-TAP** on polyimide substrates (top right) and a bottom-gate/top-contact OFET for zone-cast **TIPS-TAP** under crossed polarisers (bottom).

Table 2 Summarized electric parameters for field-effect transistors fabricated from zone-cast **TIPS-TAP**. Averaged values and standard error were obtained from a representative set of identically prepared transistors. On/off-ratios ($I_{\text{on}}/I_{\text{off}}$) were calculated for $I_{\text{on}}(V_G = 0 \text{ V})/I_{\text{off}}(V_G = 40 \text{ V})$

| Architecture | Best μ_e [cm ² V ⁻¹ s ⁻¹] | Average μ_e [cm ² V ⁻¹ s ⁻¹] | Average threshold voltage [V] | On/off ratio |
|----------------------------|--|---|-------------------------------------|----------------------------------|
| Bottom gate-top contact | 0.16 | (0.093 ± 0.005) | 14.7 ± 0.9 | 10 ⁴ –10 ⁵ |
| Bottom contact-top gate | 0.42 | (0.22 ± 0.04) | 52.7 ± 1.9 | 10 ⁴ |

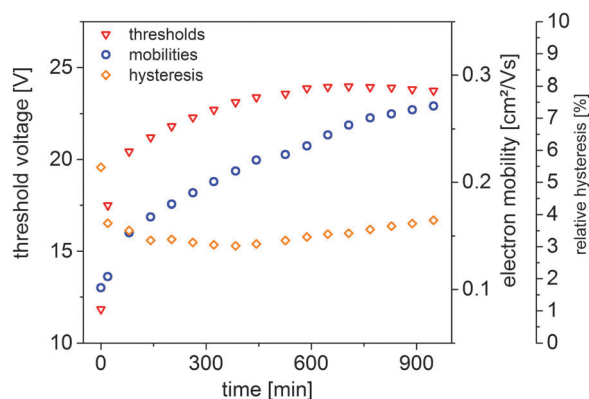


Fig. 9 Characteristic parameter of the transistor (saturation mobility, threshold voltage and relative hysteresis) as function of bias stressing time.

output characteristics (see ESI†). Upon bias stressing the electron mobility and threshold voltage increase within the first minutes and remained rather stable for the remaining time of the stress experiment. Similarly, the hysteresis of the device decreases below that of its already low initial level upon bias stressing. We attribute this behaviour to trap states being populated during the 20 minutes of positive voltage stress.

Once the trap states are populated, and no reverse bias is applied to depopulate these states, they remain populated between the different stress cycles, causing no further change in the device performance. While we do not speculate on the nature of the trap states, the sole observation of these states demonstrates the need for accurate report and analysis of the hysteresis and effects of pre-biasing on the device performance of **TIPS-TAP**. While further studies of the effect of environment and electrical biasing are required, our results indicate that **TIPS-TAP** can act as a very stable electron transporting material and is not chemically decomposed upon bias stress.

Conclusion

We have demonstrated that **TIPS-TAP** is a valuable and electrically stable electron transporting material. We report the energy levels of **TIPS-TAP** in film, measured by UPS, investigated the morphology and electrical performance of both spin-coated and zone-cast field-effect transistors and investigated their hysteresis and stability. This study shows that azaacenes can

be attractive n-channel semiconductors for a high throughput and low-cost production of electronic circuits.

Acknowledgements

We would like to thank Michael Töpper (Fraunhofer IZM, Berlin, Germany) for providing a sample of BCB Cyclotene Polymer and Prof Marcus Motzkus (PCI Heidelberg, Germany) for free access to the AFM setup. Fabian Paulus thanks the Graduate College 'Connecting Molecular π -Systems into Advanced Functional Materials' and Jens U. Engelhart the Stiftung Deutsche Telekom for scholarship. Prof Uwe Bunz thanks the DFG (Bu 771/7-1) for generous support.

References

- 1 C. Wang, H. Dong, W. Hu, Y. Liu and D. Zhu, *Chem. Rev.*, 2012, **112**, 2208–2267.
- 2 J. E. Anthony, *Angew. Chem., Int. Ed. Engl.*, 2008, **47**, 452–483.
- 3 H. Sirringhaus, *Adv. Mater.*, 2014, **26**, 1319–1335.
- 4 H. Klauk, *Chem. Soc. Rev.*, 2010, **39**, 2643–2666.
- 5 J. E. Anthony, J. S. Brooks, D. L. Eaton and S. R. Parkin, *J. Am. Chem. Soc.*, 2001, **123**, 9482–9483.
- 6 S. K. Park, T. N. Jackson, J. E. Anthony and D. a. Mourey, *Appl. Phys. Lett.*, 2007, **91**, 063514.
- 7 M. M. Payne, S. R. Parkin, J. E. Anthony, C. Kuo and T. N. Jackson, *J. Am. Chem. Soc.*, 2005, **127**, 4986–4987.
- 8 T. Sakanoue and H. Sirringhaus, *Nat. Mater.*, 2010, **9**, 736–740.
- 9 Y. Su, X. Gao, J. Liu, R. Xing and Y. Han, *Phys. Chem. Chem. Phys.*, 2013, **15**, 14396.
- 10 G. Giri, E. Verploegen, S. C. B. Mannsfeld, S. Atahan-Evrenk, D. H. Kim, S. Y. Lee, H. a. Becerril, A. Aspuru-Guzik, M. F. Toney and Z. Bao, *Nature*, 2011, **480**, 504–508.
- 11 G. Giri, S. Park, M. Vosgueritchian, M. M. Shulaker and Z. Bao, *Adv. Mater.*, 2014, **26**, 487–493.
- 12 Y. Diao, B. C.-K. Tee, G. Giri, J. Xu, D. H. Kim, H. A. Becerril, R. M. Stoltenberg, T. H. Lee, G. Xue, S. C. B. Mannsfeld and Z. Bao, *Nat. Mater.*, 2013, **12**, 665–671.
- 13 M. Ahles, R. Schmechel and H. Von Seggern, *Appl. Phys. Lett.*, 2004, **85**, 4499–4501.
- 14 M. Ahles, R. Schmechel and H. Von Seggern, *Appl. Phys. Lett.*, 2005, **87**, 85–88.
- 15 U. H. F. Bunz, J. U. Engelhart, B. D. Lindner and M. Schaffroth, *Angew. Chem., Int. Ed.*, 2013, **52**, 3810–3821.
- 16 U. H. F. Bunz, *Acc. Chem. Res.*, 2015, **48**, 1676–1686.
- 17 U. H. F. Bunz, *Chemistry*, 2009, **15**, 6780–6789.
- 18 Z. Liang, Q. Tang, R. Mao, D. Liu, J. Xu and Q. Miao, *Adv. Mater.*, 2011, **23**, 5514–5518.
- 19 Y.-Y. Liu, C.-L. Song, W.-J. Zeng, K.-G. Zhou, Z.-F. Shi, C.-B. Ma, F. Yang, H.-L. Zhang and X. Gong, *J. Am. Chem. Soc.*, 2010, **132**, 16349–16351.
- 20 C.-L. Song, C.-B. Ma, F. Yang, W.-J. Zeng, H.-L. Zhang and X. Gong, *Org. Lett.*, 2011, **13**, 2880–2883.
- 21 Q. Miao, *Adv. Mater.*, 2014, 5541–5549.

- 22 Z. Liang, Q. Tang, J. Xu and Q. Miao, *Adv. Mater.*, 2011, **23**, 1535–1539.
- 23 S. Miao, A. L. Appleton, N. Berger, S. Barlow, S. R. Marder, K. I. Hardcastle and U. H. F. Bunz, *Chemistry*, 2009, **15**, 4990–4993.
- 24 D. Liu, X. Xu, Y. Su, Z. He, J. Xu and Q. Miao, *Angew. Chem., Int. Ed. Engl.*, 2013, 6222–6227.
- 25 D. Liu, Z. He, Y. Su, Y. Diao, S. C. B. Mannsfeld, Z. Bao, J. Xu and Q. Miao, *Adv. Mater.*, 2014, **26**, 7190–7196.
- 26 Y. Qi, S. K. Mohapatra, S. Bok Kim, S. Barlow, S. R. Marder and A. Kahn, *Appl. Phys. Lett.*, 2012, **100**.
- 27 O. L. Griffith, J. E. Anthony, A. G. Jones, Y. Shu and D. L. Lichtenberger, *J. Am. Chem. Soc.*, 2012, **134**, 14185–14194.
- 28 L. Chua, J. Zaumseil, J. Chang, E. C.-W. Ou, P. K.-H. Ho, H. Sirringhaus and R. H. Friend, *Nature*, 2005, **434**, 194–199.
- 29 W. Pisula, A. Menon, M. Stepputat, I. Lieberwirth, U. Kolb, A. Tracz, H. Sirringhaus, T. Pakula and K. Müllen, *Adv. Mater.*, 2005, **17**, 684–689.
- 30 C. M. Duffy, J. W. Andreasen, D. W. Breiby, M. M. Nielsen, M. Ando, T. Minakata and H. Sirringhaus, *Chem. Mater.*, 2008, **20**, 7252–7259.